# RSC Advances

SUPPLEMENTARY INFORMATION

Investigation of the activity and stability of Pd-based catalysts towards the oxygen reduction (ORR) and evolution reactions (OER) for iron-air batteries

C. Alegre, A. Stassi, E Modica, C. Lo Vecchio, A.S. Aricò, V. Baglio

The rotating disk electrode (RDE) method was also employed for the O_2 reduction measurements at various electrode rotation rates (ω) and room temperature, using a conventional three-compartment electrochemical cell. The reference electrode was a Hg|HgO and the electrolyte was a 1 M KOH solution. This concentration was selected as a compromise between the concentration (0.1 M) usually employed for ORR studies in RDE for fuel cell applications and the one employed in metal-air batteries (6 M). The counter electrode was a high area platinum foil and the working electrode was a glassy carbon (GC) rotating disk electrode of 5 mm in which the thin film of catalysts was deposited. The 30% Pd/Vul, Pd/KB and Pt/Vul catalytic inks were prepared by sonicating each catalyst in isopropyl alcohol and 30 wt. % of Nafion solution for 30 minutes. The GC disk was firstly mirror-polished with an alumina suspension in an OP-Felt cloth. Then, several droplets of the corresponding ink were deposited onto a GC disk to obtain a final metal loading of 50 μg cm^{-2}. The system was purged with He for 30 minutes before and after each measurement. In addition, conditioning of the catalyst was carried out by triangular voltage sweeps at 100 mV s^{-1} between 0 and 1.2 V vs reference hydrogen electrode (RHE), under helium flow, for 50 cycles to obtain a stable voltammogram. Hence, 3 potential cycles were performed from 0.05 to 1.2 V vs RHE, at a scan rate of 10 mV s^{-1} until reproducible CVs were obtained. ORR activity was evaluated by linear sweep voltammetries from 1.1 to 0.2 V vs RHE, at a scan rate of 5 mV s^{-1} and different rotations per minute (rpm), and in a O_2-saturated 1M KOH solution.

Figure S.1 (a) shows the behavior of the catalysts in RDE for the ORR. The results are in good agreement with the results obtained by using a gas-diffusion working electrode (GDWE) with a practical geometrical area of 0.5 cm^2. As observed in Fig. S.1 (b), the activity for the ORR follows the same trend observed for the GDWE, i.e. Pt/Vul > Pd/KB > Pd/Vul. The current density values are lower compared to those obtained in the GDWE due to the different configuration and loading. In the RDE, oxygen must solubilize in the electrolyte and diffuse to the electrode surface. The most active catalyst in terms of onset and kinetic current (ik) values is 30% Pt/Vul. Among the two Pd-based catalysts, Pd/KB shows higher activity than Pd/Vul because of its slightly larger electrochemical surface area (ECSA), see below (Table S.1). Moreover, Pd/KB has the highest limiting current with respect to the other catalysts due to a better dispersion of the nanoparticles.
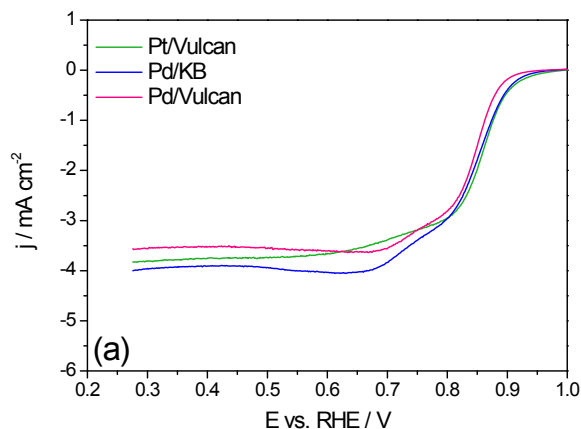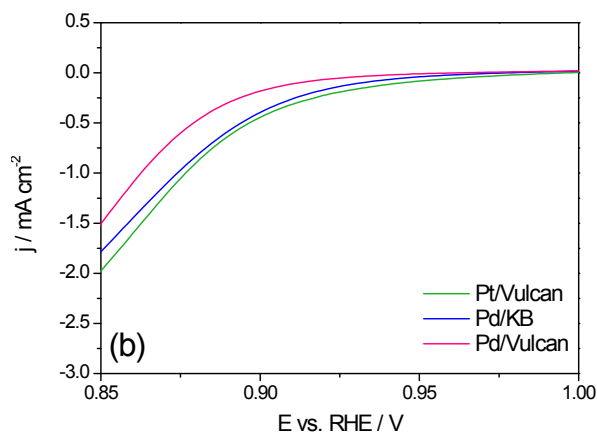
Figure S.1. (a) Comparison of RDE results on O_2 reduction for the assessed catalysts in O_2-saturated 1 M KOH solution at ω = 1600 rpm; (b) Zoom of the graph in the high potential region.

In order to establish a comparison with the literature, Pd/KB was also tested in a 0.1 M KOH solution. Figure S.2 shows the comparison of the performance towards the ORR in both solutions at 1600 rpm. A higher limit current density was obtained with the less concentrated solution (0.1 M KOH), reaching similar values to the ones reported in literature for other Pd-based catalysts for the ORR in alkaline media [22-25].
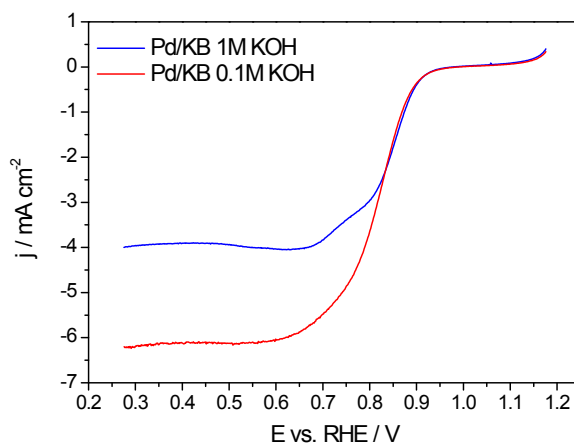

Figure S.2. (a) Comparison of RDE results on O_2 reduction for Pd/KB in O_2-saturated 0.1 M KOH and 1 M KOH solution at ω = 1600 rpm.

Table S.1 summarizes the main kinetic parameters obtained for the oxygen reduction in RDE configuration.

Table S.1. Kinetic parameters for oxygen reduction for the assessed catalysts in O_2-saturated 1M KOH solution. Ω = 1600 rpm.

| Catalyst	ECSA / $m^2\ g^{-1}$	Tafel slope I region / $mV\ dec^{-1}$	Tafel slope II region / $mV\ dec^{-1}$	$E_{1/2}$ / mV	SA at 0.85 V vs RHE / $mA\ cm^{-2}$	MA at 0.85 V vs RHE / $A\ g^{-1}$
Pt/Vulcan	44	57	231	854	0.21	92
Pd/KB	54	61	159	848	0.12	64
Pd/Vulcan	52	46	140	846	0.12	62

The ECSA for Pt/Vulcan was calculated by integrating the area under the hydrogen adsorption peak between 0.05 and 0.4 V vs RHE, whereas for Pd-based catalysts the ECSA was determined from the integration of the peak related to Pd-oxide reduction between 0.4 and 0.8 V vs RHE, assuming 405 μC cm^{-2} for the reduction of a monolayer of Pd-oxide. As expected, Pd/KB presents the highest ECSA, given the higher specific surface area (in terms of BET) of the carbon support, leading to high dispersion and lower crystallite size of Pd particles (4.0 nm). The specific activity (SA) for O_2 reduction was calculated at 0.85 V vs RHE normalizing the kinetic currents for the catalyst loading and the ECSA. The value of half-wave potential ($E_{1/2}$) indicates the capability of catalysts in reducing the ORR over-potential [26]. Pt/Vulcan presents the highest $E_{1/2}$, 854 mV, whereas both Pd catalysts present similar values, around 847 mV, indicating a poorer behavior towards the ORR, as already observed. Figure S.3 shows the Tafel plots for the three assessed catalysts. The values of Tafel slope are reported in Table S.1, taking into account two regions, at low current density values (region I) and at high current density values (region II).
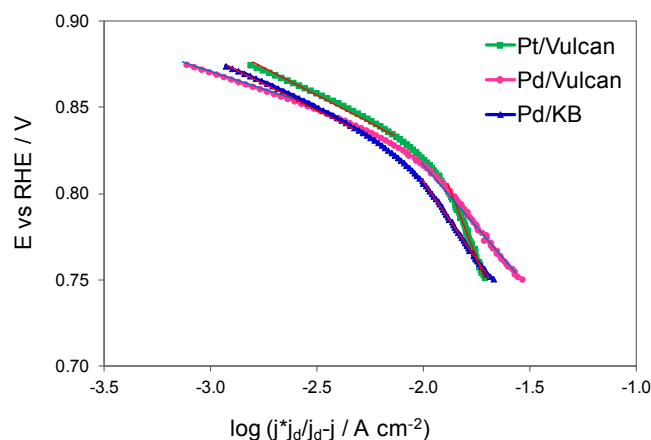
Figure S.3. Mass transfer corrected Tafel plots for the ORR on
Pt/Vulcan, Pd/KB and Pd/Vulcan in a 1M KOH solution.

TEM micrographs of the Pd-based catalysts after the cycling tests are shown in Figure S.4. Pd/Vulcan suffers a certain degree of sintering (Figure S.4 (a)) in comparison to the fresh catalyst (see Figure 2 in the manuscript). This catalyst is also affected by the Ostwald ripening process, which leads to the dissolution and re-precipitation of Pd particles on the Nafion ionomer (Figure S.4. (b)). Instead, Pd/KB presents some regions which maintain a suitable particle dispersion, Figure S.4 (c), whereas other regions show a significant presence of large agglomerates of Pd particles after the degradation tests, Figure S.4 (d). This explains the decay in performance for this catalyst.
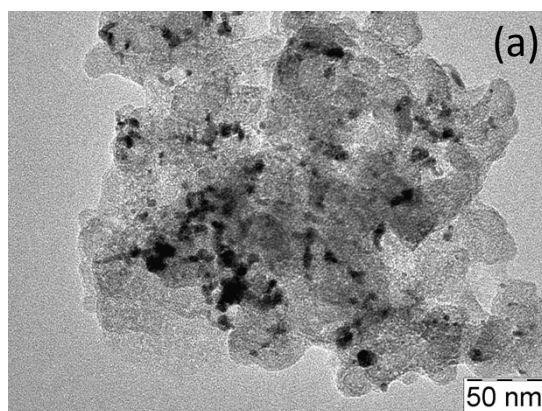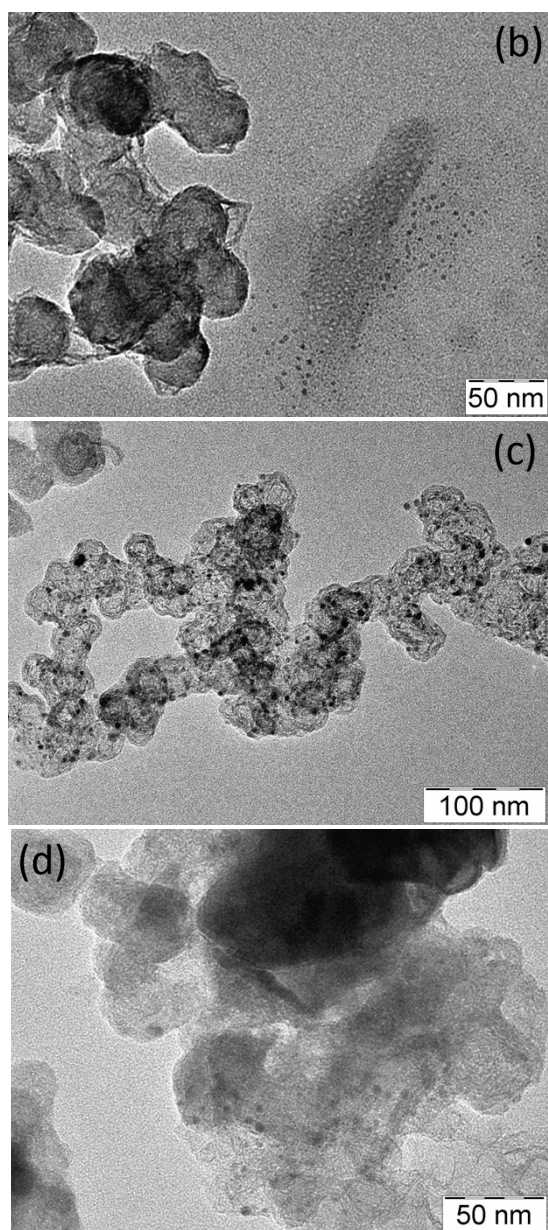
Figure S.4. TEM micrographs for (a-b) 30% Pd/Vulcan and (c-d) 30% Pd/KB after cycling tests.